Single-shot spatiotemporal measurements of high-field terahertz pulses

J. van Tilborg, C. B. Schroeder, Cs. Tóth, C. G. R. Geddes, E. Esarey, and W. P. Leemans

Lawrence Berkeley National Laboratory, University of California, Berkeley, California 94720, USA

Received August 17, 2006; revised October 26, 2006; accepted October 26, 2006;
posted October 30, 2006 (Doc. ID 74161); published January 12, 2007

The electric field profiles of broad-bandwidth coherent terahertz (THz) pulses, emitted by laser-wakefield-accelerated electron bunches, are studied. The near-single-cycle THz pulses are measured with two single-shot techniques in the temporal and spatial domains. Spectra of 0–6 THz and peak fields up to $\simeq 0.4$ MV cm^{-1} are observed. The measured field substructure demonstrates the manifestation of spatiotemporal coupling at focus, which affects the interpretation of THz radiation as a bunch diagnostic and in high-field pump–probe experiments. © 2007 Optical Society of America

OCIS codes: 020.1670, 140.7090, 320.5540.

Intense terahertz (THz) radiation, covering electromagnetic wavelengths of 10–1000 μm, is interesting for studies of ultrafast processes in semi- and superconductors. Peak THz fields of the order of MV cm^{-1} allow for use of the THz pulse as the pump beam in pump–probe experiments.[1] While conventional laser-based sources (e.g., optical rectification or a photoconductive antenna) are typically limited to generation of ≈ 50 kV cm^{-1} fields, coherent THz emission from femtosecond electron bunches has been described to yield single-cycle radiation that is potentially 1 to 2 orders of magnitude more intense.[2,3] The coherent THz radiation from such sources is also used as a temporal electron bunch diagnostic.[2,4] The results described in this Letter are based on THz emission from electron bunches produced by a laser wakefield accelerator[5] (LWFA). The LWFA delivers multi-nanocoulomb relativistic electron bunches, intrinsically synchronized to the laser pulse. Through emission of coherent transition radiation (CTR), these ultrashort bunches emit THz pulses as they exit the plasma–vacuum boundary.[3–5]

Studies of spatiotemporal field coupling[6,7] at focus have been performed with scanning techniques on conventional low-field laser-based THz sources.[8,9] Here we report on single-shot measurements of the temporal and spatial profiles of intense LWFA-produced THz pulses. The spatiotemporal coupling impacts the temporal properties of the radiation pulse and, therefore, the interpretation of LWFA-based experimental results. In addition, due to fluctuations in the LWFA performance, development of single-shot techniques is required.

The high-power Ti:Al_2O_3 laser of the Lasers, Optics and Accelerator Systems Integrated Studies (LOASIS) facility[5] at the Lawrence Berkeley National Laboratory was used for the experiments. In the experiment, an electron bunch with a total charge of $\simeq 2$ nC was produced, while its energy distribution $g(E)$ was measured to be of the form $g(E) \propto \exp(-E/E_t)$, with $E_t = 5$ MeV. THz radiation was emitted as the electrons propagated through the dielectric discontinuity of the plasma–vacuum boundary.[3–5] Two variations of the electro-optic sampling (EOS) technique were operated to characterize the LWFA-produced THz pulses, namely, a single-shot temporal cross-correlation technique[10,11] and a single-shot two-dimensional (2D) spatial technique.[12]

An $f/2$ 90° off-axis parabola (OAP2, 15 cm focal length), positioned off center ($\theta = 19°$ with respect to the main axis), was used to collect and collimate a portion of the emitted THz radiation (see Fig. 1). The collimated THz radiation was focused by an $f/2.4$ 90° off-axis parabola (OAP3, 18 cm focal length) onto a 200 μm thick GaP crystal outside the target chamber [through a polyethylene (PE) window].

For the single-shot temporal EOS technique, two laser beams, both with a minimum pulse length of 70 fs (intensity FWHM), were split off from the main laser beam, conserving synchronization. The first probe beam, $I_1(t)$ in Fig. 1, was stretched (chirped) to a length of 1350 fs (intensity FWHM). After propagation through a polarizer, the laser pulse was focused (spot size < 20 μm) to overlap with the THz beam in

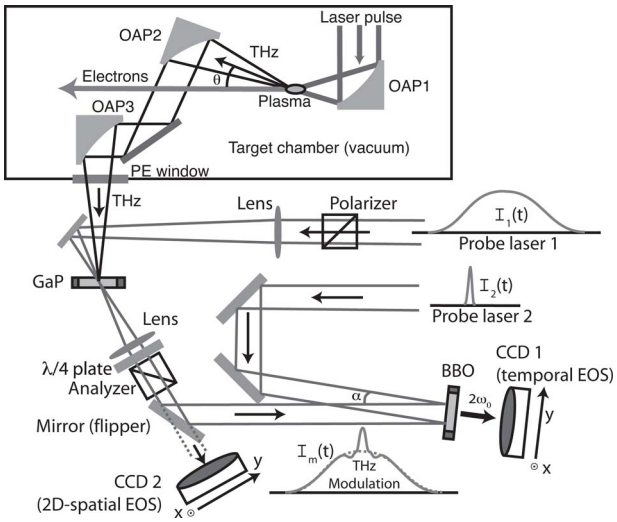

Fig. 1. Schematic representation of the LWFA, the THz (CTR) beam path, and the two EOS detection setups (temporal and 2D spatial). Abbreviations defined in text.

0146-9592/07/030313-3/$15.00

the (110)-cut GaP. A $\lambda/4$ plate was rotated to yield a circular polarization state incident on the analyzer.

Through the THz-induced electro-optic (EO) effect in the GaP crystal, the intensity envelope of probe laser $I_1(t)$, transmitted through the analyzer, was modulated to $I_m(t)$. It can be shown[13] that $I_m(t) = 1/2[1+\sin\Gamma^*(t)]I_1(t)$, where in the Fourier domain $\Gamma^*(\nu)=\Gamma_{\mathrm{THz}}(\nu)T_{\mathrm{GaP}}(\nu)$ and ν is the radiation frequency. $\Gamma^*(\nu)$ represents the THz-induced phase retardation and is a convolution of the source profile $\Gamma_{\mathrm{THz}}(\nu)$ and crystal effects $T_{\mathrm{GaP}}(\nu)$.[13,14] The function $T_{\mathrm{GaP}}(\nu)$ for 200 μm thick GaP has previously been discussed[15]; over the frequency range 0–8 THz, dispersion effects were found to be relatively limited. $\Gamma_{\mathrm{THz}}(t)$ is related to the original THz field profile $E_{\mathrm{THz}}(t)$ through[14] $\Gamma_{\mathrm{THz}}(t)=2\pi L n_0^3 r_{41}E_{\mathrm{THz}}(t)/\lambda_0$, with $L=200$ μm the GaP crystal thickness, $n_0=3.19$ the index of refraction in GaP at λ_0, and $r_{41}\simeq 2\times10^{-12}$ mV^{-1} the EO coefficient of GaP.[16] For CTR, the THz field $E_{\mathrm{THz}}(\nu)$ is determined by the Fourier transformation of the electron bunch charge profile and diffraction effects from the limited size of the transverse plasma–vacuum interface.[3,15]

The EO-modulated laser envelope was recorded in a single-shot manner[10] through noncollinear sum-frequency generation of $I_m(t)$ and a second short laser pulse $I_2(t-\tau_2)$ (pulse length of 70 fs FWHM, which determines the time resolution of the system), with τ_2 the respective temporal delay between both laser beams. The frequency doubling occurred in a β-barium borate (BBO) crystal. A CCD camera [CCD 1 (see Fig. 1)] recorded the time-integrated transverse (xy-plane) intensity distribution of the frequency-doubled radiation $I_{2\omega}(x,y)$. During post-processing, each image $I_{2\omega}(x,y)$ was integrated over x to yield $I_{2\omega}(y)$. Also, each profile was normalized to yield $I_{2\omega}\rightarrow(I_{2\omega}-I_{2\omega,0})/I_{2\omega,0}$, with $I_{2\omega,0}$ the reference profile in absence of a THz pulse. Due to the noncollinear geometry, the delay τ_2 is a function of the position y within the crystal and $I_{2\omega}(y)$ can be converted to a temporal profile $I_{2\omega}(\tau_2)$ through $\tau_2=(y/c)\tan(\alpha^*/2)$, with c the speed of light in vacuum. The angle of incidence between both laser pulses at the crystal surface was $\alpha=10°$ (inside the BBO crystal $\alpha^*=6.3°$), and the laser beam diameters were $\simeq$6 mm (intensity FWHM). After defining a measured retardation function as $\Gamma_{\mathrm{cor}}(\tau_2)=\arcsin I_{2\omega}(\tau_2)$, it can be found[13,14,17] that

$$\Gamma_{\mathrm{cor}}(\nu)\simeq\Gamma_{\mathrm{THz}}(\nu)T_{\mathrm{GaP}}(\nu)I_{\mathrm{env},2}(\nu), \qquad (1)$$

with $I_{\mathrm{env},2}(\nu)$ the envelope spectrum of $I_2(t)$.

Three measured representative phase retardation profiles $\Gamma_{\mathrm{cor}}(t)$ and $|\Gamma_{\mathrm{cor}}(\nu)|$, obtained through the single-shot measurement of $I_{2\omega}(\tau_2)$, are shown in Figs. 2(a) and 2(b), respectively. Shot A in Fig. 2(a) shows a field profile with just one main field cycle (spectrum extending to $\simeq$6 THz) and peak phase retardation of $\Gamma_{\mathrm{cor}}\simeq1$ rad. Through relation (1), and considering that the field reducing effects of dispersion and surface transmission in the GaP crystal can be approximated as $T_{\mathrm{GaP}}\simeq0.25$,[15] an estimation of

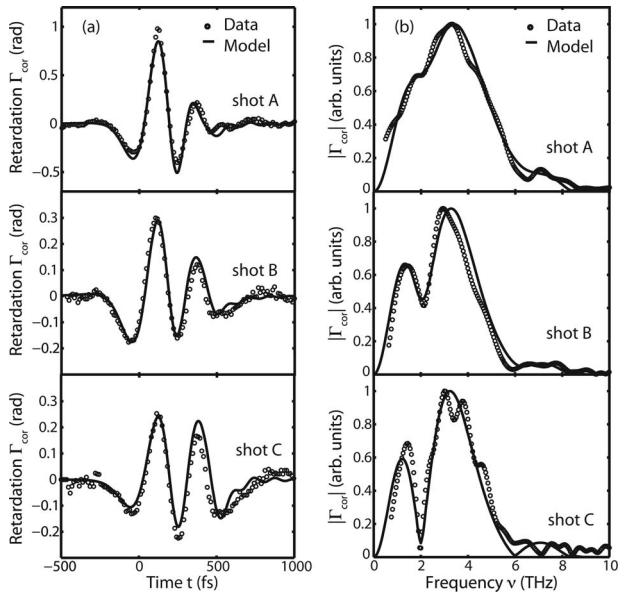

Fig. 2. (a) Measured single-shot THz field profiles in terms of phase retardation $\Gamma_{\mathrm{cor}}(t)$. (b) Fourier transformation $|\Gamma_{\mathrm{cor}}(\nu)|$ of the data. The solid curves are calculated from a CTR-based model.

the THz field amplitude at the crystal location yields $E_{\mathrm{THz}}\simeq0.4$ MV cm^{-1}. The estimated sensitivity (based on fluctuation of $I_{2\omega,0}$) is $\simeq$20 kV cm^{-1}.

Figure 2 also displays the presence of a trailing THz pulse (two maxima in the temporal domain and interference in the spectral domain, more clearly visible in shots B and C). Although the position of the trailing pulse was relatively stable at a delay of 230–250 fs, its relative field strength showed strong fluctuations (from weaker in shot A to stronger in shot C). Each measurement (in both domains) was compared with modeled[4,15] EOS profile, which yielded best agreement if a 45 fs (rms) electron bunch was assumed (one bunch emitting two THz pulses at a separation of 240 fs). The relative field amplitude of the modeled trailing pulse was 30%, 57%, and 90% for shots A, B, and C, respectively.

For single-shot 2D-spatial THz imaging, the setup in Fig. 1 was slightly modified. The $\lambda/4$ plate and the two lenses in the path of probe laser 1 were removed, such that a collimated laser beam was overfilling the THz spot at the GaP crystal. By removing the flipper-mirror, the 2D time-integrated intensity distribution $I_{2\mathrm{D}}(x,y,\tau)$ was recorded by CCD camera 2, with τ the delay between $E_{\mathrm{THz}}(t)$ and $I_1(t)$. The compressor for probe laser 1 was tuned to yield a pulse length of 70 fs (intensity FWHM), which allowed for time-resolved 2D imaging. For a linear-polarized laser beam, it can be derived[13,14] that $I_{2\mathrm{D}}(x,y,\tau)\propto\int I_1(t-\tau)\sin^2[\Gamma^*(x,y,t)/2]\mathrm{d}t$, with $\Gamma^*(\nu)$ previously defined in the Fourier domain.

After switching the setup to the single-shot 2D EOS technique, the 2D laser transmission $I_{2\mathrm{D}}(x,y,\tau)$ was recorded while varying the delay τ between the laser and THz beam. It was found that the 2D THz profile was stable at a given delay, but evolved over time. Three characteristic $I_{2\mathrm{D}}(x,y,\tau)$ images are shown in Figs. 3(a)–3(c), with (a) $\tau=-250$ fs, (b) τ

=0 fs, and (c) τ=350 fs. The data show that a main THz spot is present [see, e.g., Fig. 3(b)], where the main spot has an intensity FWHM of ≃600 μm. The substructure indicates the presence of effects from diffraction [e.g., shot D in Fig. 3(a)], coma [e.g., shot F in Fig. 3(c)], and other aberrations. Diffraction is present because the THz emission overfills parabola OAP2 (see Fig. 1), while coma can be present if the alignment of OAP2 and OAP3 is not perfect. At a fixed delay τ=0 fs, another series of images was analyzed by taking lineouts at y=0 mm; several lineouts, shown in Fig. 4, indicate that the position of the substructure is stable, but that the relative intensity fluctuates shot to shot.

It was found that it is unlikely that the double-THz-pulse structure (e.g., EOS measurements in Fig. 2) is a result of the LWFA production of two electron bunches as previously hypothesized.[15] The absence of a correlation between the THz-pulse features with LWFA parameters such as electron energy and plasma density supports this conclusion. The double-THz-pulse profile is rather the result of optical effects in the THz focusing system (diffraction, coma, and other aberrations). A heuristic ray-based model (excluding effects such as the Gouy shift and bandwidth-induced dispersion at focus), where each ray was defined as a single-cycle pulse with a finite transverse dimension, was developed and confirmed coma-induced occurrence of a double-pulse profile.[17] Experimentally, the spatiotemporal coupling is fixed by the arrangement and alignment of the optics in the THz beam line, resulting in a stable positioning of the temporal and spatial substructure (see Figs. 2 and 4). However, fluctuations of the electron bunch energy and pointing can result in a varying angular THz emission profile, which yields fluctuations in the amplitude ratio of the field structure.

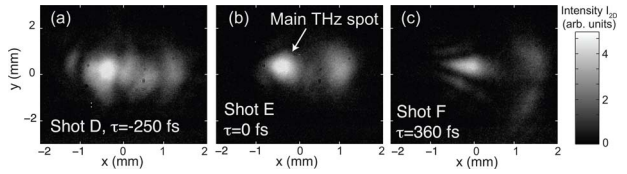

Fig. 3. (Color online) Three representative single-shot 2D THz images $I_{2D}(x,y,\tau)$, taken at different values for the delay τ between the THz and laser pulse.

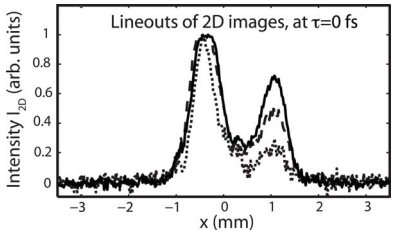

Fig. 4. At a fixed delay τ=0 fs, lineouts at y=0 of three consecutive 2D shots are displayed.

In summary, single-cycle broad-bandwidth THz pulses were studied at focus, demonstrating the production of THz pulses with spectra of 0–6 THz and peak fields of ≃0.4 MV cm^{-1}. A trailing THz pulse, with varying amplitude shot to shot, was observed at a stable separation of ≃240 fs. A 2D-spatial EOS technique indicated the presence of a main THz spot surrounded by time-evolving substructure. Both techniques support the conclusion that diffraction, coma, and other aberrations are spatiotemporally coupled in the focal volume.

This work was supported by the U.S. Department of Energy under contract DE-AC02-05CH11231. J. van Tilborg's e-mail address is JvanTilborg@lbl.gov.

References

1. M. S. Sherwin, C. A. Schmuttenmaer, and P. H. Bucksbaum, eds., *Opportunities in THz Science* (DOE-NSF-NIH workshop, 2004).
2. G. L. Carr, M. C. Martin, W. R. McKinney, K. Jordan, G. R. Neil, and G. P. Williams, Nature **420**, 153 (2002).
3. C. B. Schroeder, E. Esarey, J. van Tilborg, and W. P. Leemans, Phys. Rev. E **69**, 016501 (2004).
4. J. van Tilborg, C. B. Schroeder, C. V. Filip, Cs. Tóth, C. G. R. Geddes, G. Fubiani, R. Huber, R. A. Kaindl, E. Esarey, and W. P. Leemans, Phys. Rev. Lett. **96**, 014801 (2006).
5. W. P. Leemans, C. G. R. Geddes, J. Faure, Cs. Tóth, J. van Tilborg, C. B. Schroeder, E. Esarey, G. Fubiani, D. Auerbach, B. Marcelis, M. A. Carnahan, R. A. Kaindl, J. Byrd, and M. C. Martin, Phys. Rev. Lett. **91**, 074802 (2003).
6. M. Kempe and W. Rudolph, Phys. Rev. A **48**, 4721 (1993).
7. M. A. Porras, Phys. Rev. E **65**, 026606 (2002).
8. S. Hunsche, S. Feng, H. G. Winful, A. Leitenstorfer, M. C. Nuss, and E. P. Ippen, J. Opt. Soc. Am. A **16**, 2025 (1999).
9. Z. Jiang and X.-C. Zhang, Opt. Express **5**, 243 (1999).
10. S. P. Jamison, J. Shen, A. M. MacLeod, W. A. Gillespie, and D. A. Jaroszynski, Opt. Lett. **28**, 1710 (2003).
11. S. P. Jamison, G. Berden, A. M. MacLeod, D. A. Jaroszynski, B. Redlich, A. F. G. van der Meer, and W. A. Gillespie, Nucl. Instrum. Methods Phys. Res. A **557**, 305 (2006).
12. Q. Wu, T. D. Hewitt, and X.-C. Zhang, Appl. Phys. Lett. **69**, 1026 (1996).
13. G. Gallot and D. Grischkowsky, J. Opt. Soc. Am. B **16**, 1204 (1999).
14. J. Faure, J. van Tilborg, R. A. Kaindl, and W. P. Leemans, Opt. Quantum Electron. **36**, 681 (2004).
15. J. van Tilborg, C. B. Schroeder, C. V. Filip, Cs. Tóth, C. G. R. Geddes, G. Fubiani, E. Esarey, and W. P. Leemans, Phys. Plasmas **13**, 056704 (2006).
16. Q. Wu and X.-C. Zhang, Appl. Phys. Lett. **70**, 1784 (1997).
17. J. van Tilborg, "Coherent terahertz radiation from laser-wakefield-accelerated electron beams," Ph.D. thesis (Eindhoven University of Technology, 2006).